Numerical analysis of $In_{0.53}Ga_{0.47}As/InP$ single photon avalanche diodes*

Zhou Peng(周 鹏)[a], Li Chun-Fei(李淳飞)[a]†, Liao Chang-Jun(廖常俊)[b], Wei Zheng-Jun(魏正军)[b], and Yuan Shu-Qiong(袁书琼)[b]

[a] *Department of Physics, Harbin Institute of Technology, Harbin* 150001, *China*

[b] *Laboratory of Photonic Information Technology, School for Information and Optoelectronic Science and Engineering, South China Normal University, Guangzhou* 510631, *China*

(Received 30 June 2010; revised manuscript received 19 August 2010)

A rigorous theoretical model for $In_{0.53}Ga_{0.47}As/InP$ single photon avalanche diode is utilized to investigate the dependences of single photon quantum efficiency and dark count probability on structure and operation condition. In the model, low field impact ionizations in charge and absorption layers are allowed, while avalanche breakdown can occur only in the multiplication layer. The origin of dark counts is discussed and the results indicate that the dominant mechanism that gives rise to dark counts depends on both device structure and operating condition. When the multiplication layer is thicker than a critical thickness or the temperature is higher than a critical value, generation–recombination in the absorption layer is the dominative mechanism; otherwise band-to-band tunneling in the multiplication layer dominates the dark counts. The thicknesses of charge and multiplication layers greatly affect the dark count and the peak single photon quantum efficiency and increasing the multiplication layer width may reduce the dark count probability and increase the peak single photon quantum efficiency. However, when the multiplication layer width exceeds 1 μm, the peak single photon quantum efficiency increases slowly and it is finally saturated at the quantum efficiency of the single photon avalanche diodes.

Keywords: single photon avalanche diodes, gate-mode, single photon quantum efficiency, dark count probability

PACS: 85.30.De, 85.60.Dw, 85.60.Gz **DOI:** 10.1088/1674-1056/20/2/028502

1. Introduction

Single photon detectors are increasingly needed in the emerging fields of quantum computation and quantum cryptography, as well as in more traditional fields that require single photon sensitivity. As in the telecom wavelengths of 1.31 μm and 1.55 μm, a separate absorption, grading, charge and multiplication (SAGCM) $In_{0.53}Ga_{0.47}As/InP$ avalanche photodiode (APD) that is reverse-biased beyond breakdown voltage (V_B) and operated in so-called Geiger mode is regarded as one of the most practical single photon detectors.[1] These APDs are also known as Geiger mode avalanche photodiodes or single photon avalanche diodes (SPADs).[2] Most of the previous experimental research has focused on commercially available APDs which are designed for use in linear mode.[3–5] In recent years, to maintain higher single photon quantum efficiency (SPQE) E_s, lower dark count probability (P_d) and better time response, SPADs designed specially for single photon detection have attracted much interest.[6–8]

SPADs are mostly concerned with single photon quantum efficiency E_s and dark count probability (P_d). In order to optimize structure design and operation of SPADs, it is necessary to clarify the mechanisms that give rise to dark count and the dependences of E_s and P_d on structure and temperature. The origin of dark count in an $In_{0.53}Ga_{0.47}As/In_{0.52}Al_{0.48}As$ SPAD with a multiplication layer width (W_m) of 0.4 μm was investigated,[9] showing that band-to-band tunneling in the multiplication layer dominated the dark count in the structure with thin multiplication layer. As for a thicker $In_{0.53}Ga_{0.47}As/InP$ SPAD with W_m of $\sim$1 μm, the most important mechanism of dark count is the generation–recombination in the absorption layer when the SPAD operated at temperatures above 240 K.[7]

*Project supported by the National Basic Research Program of China (Grant Nos. G2001039302 and 007CB307001), and the Guangdong Provincial Key Technology Research and Development Program, China (Grant No. 2007B010400009).

†Corresponding author. E-mail: cfli@hit.edu.cn

© 2011 Chinese Physical Society and IOP Publishing Ltd

In the present paper, E_s and P_d of SAGCM SPADs are numerically analysed in a wide range of multiplication and charge layers at different temperatures. The SPADs are operated in gate-mode, which is an effective method to avoid high dark count and afterpulse probability by adjusting the short gate pulse delay to synchronize with the arrival of photons. In the calculation, impact ionizations in the charge and absorption layers are taken into account in order to reflect their contribution to the avalanche breakdown, which can only take place in the multiplication region. The avalanche breakdown is analysed using a history-dependent analytical impact ionization model.[10] The history-dependent ionization coefficients with temperatures of InP[11] and $In_{0.53}Ga_{0.47}As$[12] are used.

2. Model

Figure 1 shows an SAGCM SPAD to be calculated. This SPAD consists of a 2-μm n^--doped $In_{0.53}Ga_{0.47}As$ as an absorption layer with a doping density of 1×10^{15} cm^{-3}, a multiplication layer width ranging from 0.2 μm to 3 μm, n^--doped at 1×10^{15} cm^{-3} and a charge layer doped at 1×10^{17} cm^{-3}, which is needed to reduce the electric field from the InP multiplication layer to the $In_{0.53}Ga_{0.47}As$ as an absorption region. The valence-band discontinuity between the wider gap InP (1.35 eV) and the narrow gap $In_{0.53}Ga_{0.47}As$ (0.73 eV) restricts the transportation of holes. Therefore, a quaternary material, InGaAsP, which has an intermediate bandgap between bandgaps of the InP and $In_{0.53}Ga_{0.47}As$, is grown between the $In_{0.53}Ga_{0.47}As$ and InP layers to grade the valence-band discontinuity. As a result, the transition rate of the holes is increased. For simplicity, the InGaAsP grading layer can be regarded as a part of absorption layer in the calculation.

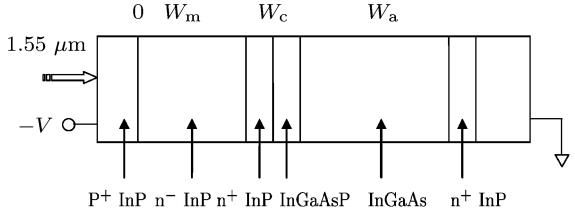


Fig. 1. Schematic of simulated SPAD structure.

Under Geiger mode operation, a high electric field, large enough to cause avalanche breakdown, is present in the InP multiplication layer. A single photon injected into the SPAD passes through the InP and the InGaAsP layers, is absorbed in the $In_{0.53}Ga_{0.47}As$ absorption layer and converted into an electron–hole carrier pair. Then, the photon-generated hole undergoes drift due to the action of the electric field, thereby depleting the $In_{0.53}Ga_{0.47}As$ absorption layer. It may increase its population because of the field-induced impact ionizations in the absorption, grading and charge layers during the way to the InP multiplication layer, thereby leading finally to breakdown there. A macroscopic current pulse is then present, indicating the arrival of the single photon.

The widths of the charge layer and the absorption layer are represented as W_c and W_a, respectively. Let $P_e(x)$ denote the probability with which an electron generated at location x triggers an avalanche breakdown. Similarly, $P_h(x)$ represents the probability with which a hole generated at location x triggers an avalanche breakdown. The E_s is commonly defined as the probability with which a photon-generated carrier rather than a dark carrier triggers an avalanche breakdown in the SPAD.[13,14] When the error rate due to afterpulse is relatively low, E_s can be approximated by[13]

$$E_s = \frac{(1 - P_d)P_{ph}}{P_o}, \tag{1}$$

where P_{ph} is the probability with which the photon-carrier starts the breakdown and P_o is the probability with which an incident optical pulse contains at least one photon. Assume that the Poisson statistic P_o can be expressed as

$$P_o = 1 - \exp(-N_o), \tag{2}$$

where N_o is the average number of photons contained in the photo pulse. Similarly, P_{ph} is assumed to be able to be represented as

$$P_{ph} = 1 - \exp(-\eta N_o P_h(W_m)), \tag{3}$$

where P_h (W_m) is the pure hole injected breakdown probability, η is the quantum efficiency of the SPAD, which is the probability with which an incident photon is absorbed and converted to an electron–hole pair in the absorber. By ignoring the incident light loss due to reflection,

$$\eta = 1 - \exp(-\alpha W_a'), \tag{4}$$

where α is the absorption coefficient of the $In_{0.53}Ga_{0.47}As$ absorber, it is 0.68×10^4 cm^{-1} for the absorber thickness 1.55 μm,[15] and W_a' is the depth of absorption layer depleted by electric field.

In order to obtain a single photon with high probability, $N_{\rm o}$ should be much smaller than 1. Therefore

$$E_{\rm s} = (1 - P_{\rm d})\eta P_{\rm h}(W_{\rm m}). \tag{5}$$

To detect a dark count, two statistically independent events should happen: (i) no less than one dark carrier created in the SPAD due to different mechanisms and (ii) dark carriers undergo drift, under the action of the electric field, to the multiplication layer and cause breakdown. By following the Poisson statistics assumption, the dark count probability $P_{\rm d}$ is commonly presented as

$$P_{\rm d} = 1 - \exp(-N_{\rm d}P_{\rm b}), \tag{6}$$

where $N_{\rm d}$ is the average number of dark carriers injected into the multiplication layer and $P_{\rm b}$ is the breakdown probability initiated by dark carriers.

However, we should note that due to the location where the initial dark carrier is created, $P_{\rm b}$ should be in different forms at different locations. Carriers generated in the charge layer and the absorption layer will be injected into the multiplication layer due to field induced drift, so that we can assume that they have the same breakdown probability as that of photo carriers, that is, $P_{\rm b} = P_{\rm h}(W_{\rm m})$. On the other hand, carriers created in the multiplication layer may be randomly distributed in the whole region. Therefore the breakdown probability should be[14]

$$\begin{aligned} P_{\rm b}(x) &= 1 - (1 - P_{\rm e}(x))(1 - P_{\rm h}(x)) \\ &= P_{\rm e}(x) + P_{\rm h}(x) - P_{\rm e}(x)P_{\rm h}(x). \end{aligned} \tag{7}$$

Another fact that should be noted is that dark carriers generated outside the multiplication region must be subjected to the multiplication effect when carriers drift through the route to the multiplication region. Therefore, dark count probabilities, owing to carriers created inside and outside the multiplication layer, should be respectively represented as

$$P_{\rm d,m} = 1 - \exp\left(-\int_0^{W_{\rm m}} {\rm d}x G_{\rm d}(x)P_{\rm b}(x)A{\cdot}\Delta t\right), \tag{8}$$

$$\begin{aligned} P_{\rm d,c-a} = 1 - \exp\Bigg(&- P_{\rm h}(W_{\rm m})A \cdot \Delta t \\ &\times \int_{W_{\rm m}}^{y} {\rm d}x G_{\rm d}(x)M(x)\Bigg), \end{aligned} \tag{9}$$

where $G_{\rm d}(x)$ is the generation rate of the dark carriers, Δt is the duration of the gate pulse, A is the area of multiplication layer, $M(x)$ is the distributed multiplication factor and y denotes the location where the carriers are generated.

$G_{\rm d}(x)$ varies with the mechanism responsible for the creation of initial dark carriers. The mechanisms generally considered are[16] diffusion from quasi-neutral regions, generation–recombination in the depletion region, tunneling and surface leakage. The diffusion and the leakage components are very small and can be neglected, thus dark counts arising from the tunneling and generation–recombination will be included in the calculation. As these two types of carriers are generated in independent locations, their dark count probabilities can be rewritten correspondingly as

$$\begin{aligned} P_{\rm d,m} = 1 - \exp\Bigg(&-N_{\rm d,m}\frac{1}{W_{\rm m}}\int_0^{W_{\rm m}} {\rm d}x(P_{\rm e}(x) \\ &+ P_{\rm h}(x) - P_{\rm e}(x)P_{\rm h}(x))\Bigg), \end{aligned} \tag{10}$$

with $N_{\rm d,m} = G_{\rm d} \cdot A \cdot W_{\rm m} \cdot \Delta t$,

$$\begin{aligned} P_{\rm d,c-a} = 1 - \exp\Bigg(&- N_{\rm d,c-a}P_{\rm h}(W_{\rm m})\frac{1}{y - W_{\rm m}} \\ &\times \int_{W_{\rm m}}^{y} {\rm d}x M(x)\Bigg), \end{aligned} \tag{11}$$

with $N_{\rm d,c-a} = G_{\rm d} \cdot A \cdot (y - W_{\rm m}) \cdot \Delta t$. Expression of $G_{\rm d}$ depends on mechanism that gives rise to it. In a reverse-biased SPAD, the generation rate of dark carriers from tunneling can be represented as[17]

$$G_{\rm d,t} = \gamma \exp(-\theta m_0^{1/2}\varepsilon_g^{3/2}/q\hbar E_{\rm m}). \tag{12}$$

For band-to-band tunneling

$$\gamma = \left(\frac{2m^*}{\varepsilon_{\rm g}}\right)^{1/2} q^2 E_{\rm m} V/(4\pi^2\hbar^2), \tag{13}$$

where m_0, m^*, $\varepsilon_{\rm g}$, q, $\hbar$, and $E_{\rm m}$ are free electron mass, tunneling effective mass, band gap, electron charge, reduced Planck constant and maximum junction electric field, respectively; θ depends on the shape detail of the barrier. For the $In_{0.53}Ga_{0.47}As$ absorber, $\theta = 0.3$ is chosen according to the experimental data,[18] and for InP multiplication layer,

$$\theta = \frac{\pi}{2\sqrt{2}}\left(\frac{m^*}{m_0}\right)^{1/2} \tag{14}$$

with the parabolic barrier assumed as an approximation.

$G_{\rm d}$ due to the generation–recombination via traps near the middle of the band gap is[19]

$$G_{\rm d,gr} = \frac{n_i}{\tau} = \frac{(N_{\rm c}N_v)^{1/2}}{\tau}\exp\left(-\frac{\varepsilon_{\rm g}}{2kT}\right), \tag{15}$$

where n_i, N_c, N_v, W and k are the intrinsic carrier concentration, effective densities of the states in the conduction and valence bands of the semiconductor, the depletion region width and the Boltzmann constant, respectively. The temperature dependences of the band gap of InP in Ref. [20] and $In_{0.53}Ga_{0.47}As$ in Ref. [21] are used.

Therefore the total dark count probability can be represented as

$$P_d = 1 - \prod_i (1 - P_{di}), \tag{16}$$

where i indicates the type of mechanism and region where the dark carriers are generated in the SPAD.

3. Calculation and results

Figure 2 shows the calculated dark count probabilities when E_s is 40%, the temperature is 223 K (−50 °C) which can be easily achieved by thermoelectric cooling. Total dark count probability P_d, dark count probability due to generation–recombination from absorption layer (P_{dgra}), probability due to tunneling from multiplication (P_{dtm}) and probability due to tunneling from the charge layer (P_{dtc}) are illustrated each as a function of multiplication layer width. Dark count probabilities from other mechanisms are too small and they are not included. In order to avoid significant tunneling in the $In_{0.53}Ga_{0.47}As$ absorption layer and to make a point of all photon-generated carrier drift into the multiplication layer with their saturation velocities, charge layer width W_c is controlled to ensure that the maximum electric field in the absorption layer E_a reaches 1.5×10^5 V/cm. For W_m ranging from 0.2 μm to 3 μm, W_c decreases from 0.33 μm to 0.14 μm. As shown in the figure, the P_d decreases sharply with the increase of multiplication layer width when $W_m < 1.2$ μm; as W_m is over 1.2 μm, its decrease becomes very slow. In another model,[11] P_d rises with W_m slightly when $W_m > 3$ μm.

At this temperature, when W_m is increased from 0.4 μm to 1.25 μm, dark count probability from tunneling in the multiplication layer is much higher than those from other mechanisms. As $W_m < 0.4$ μm, due to the high field and relatively thick charge layer, P_{dtc} is considerable. In addition, when W_m is over 1.25 μm, P_{dgra} becomes larger than P_{dtm}, generation–recombination in the absorption layer is the dominant mechanism of dark counts. It can also be seen in the figure that to maintain the same E_s, the total dark count rate of a SPAD with thin multiplication layer is much higher than that with thicker multiplication layer. This is because of the large tunnelings in the multiplication layer and the charge layer of the SPAD. A previous experimental study[9] has proven that the dark count of a SAGCM SPAD with 0.4 μm originates from the tunneling effect in the multiplication layer, which accords well with the calculation.

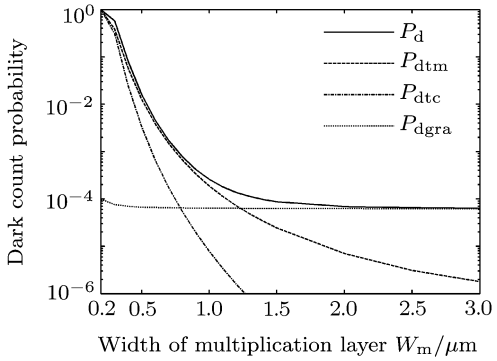


Fig. 2. Dark count probabilities each as a function of multiplication layer width at a temperature of 223 K, with E_s being 0.4.

Both E_s and P_d vary with the applied voltage, since a high electric field enhances breakdown probability and tunneling in the SPAD. Figure 3 shows dark count probabilities each as a function of E_s, with W_m and W_c being 1 μm and 0.2 μm, respectively. As shown in the figure, P_d exponentially increases with E_s and P_d is found to be 5.1×10^{-4} at E_s of 0.5. When E_s is lower than 0.14, the dark count probability caused by generation–recombination is larger than that from other mechanisms, while as E_s is over 0.14, P_{dtm} begins to exceed P_{dgra}, which indicates that band-to-band tunneling becomes the dominative mechanism of the dark counts.

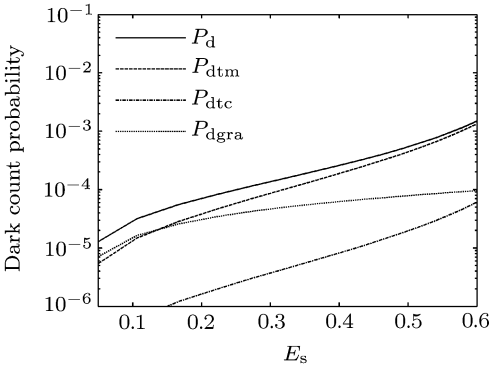


Fig. 3. Dark count probabilities each as a function of E_s at temperature of 223 K, with W_m and W_c being 1 μm and 0.2 μm, respectively.

Dark carriers from generation–recombination increase exponentially with temperature, so does

the dark count probability from generation–recombination. Figure 4 shows the dark count probabilities, each as a function of temperature for the SPAD with W_m of 1 μm which achieves good E_s and dark count performance.[6,7] P_{dtm} is over 20 times higher than P_{dtc} in a temperature range from 200 K to 300 K. When the temperature is below 233 K, P_{dtm} is higher than P_{dgra} and the tunneling in multiplication layer is the dominative mechanism of dark counts; when the temperature is above 233 K, P_{dgra} begins to exceed P_{dtm} and when the temperature is above 240 K, generation–recombination from absorption layer dominates the dark counts. In Ref. [7], an SAGCM $In_{0.53}Ga_{0.47}As$/InP SPAD with an absorber layer of $\sim$2 μm and a multiplication layer of $\sim$ 1 μm was grown and tested, and the experimental results showed that when the temperature was increased from 160 K to 240 K, tunneling in the multiplication layer is the dominative mechanism. When the temperature was increased from 240 K to 297 K, generation–recombination from the absorber became the most important mechanism. Our calculations are in agreement with the experimental results.

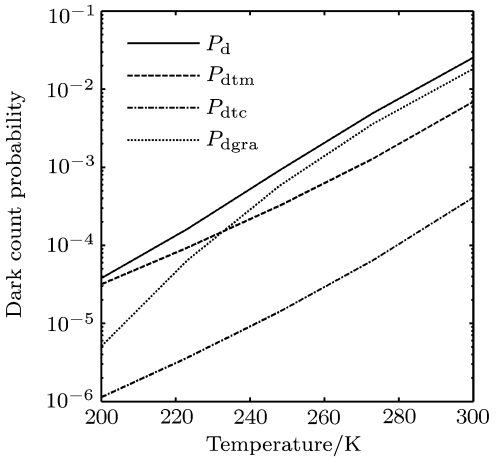


Fig. 4. Dark count probabilities each as a function of temperature, with W_m and E_s being 1 μm and 0.4 respectively.

The thickness of the charge layer greatly affects E_s and P_d, and should be carefully designed. As shown in Fig. 5, the calculated E_s and P_d of a 1-μm SPAD are each plotted as a function of W_c, with the maximum value of electric field E_m in the multiplication layer fixed to be constant. When W_c is less than 0.120 μm, P_b is close to 1 because the electric fields in charge and absorption layer are too high, causing strong tunneling in these layers. Therefore, the E_s is close to 0. As W_c increases from 0.120 μm to 0.164 μm, P_d decreases sharply, while E_s rises to 0.4. When W_c further increases to 0.270 μm, the E_s is saturated at 0.4, although P_d still decreases quickly for a while and then stays at 3.5×10^{-4}. This is because P_h (W_m) is constant and the absorption layer is fully depleted. Therefore, η is invariable and E_s is a constant. When W_c is increased from 0.270 μm to 0.290 μm, the absorption layer is not fully depleted and η drops to 0. Thus E_s drops to 0, and P_d also decreases because the dark carrier created in the absorber cannot drift into the multiplication layer. To maintain a considerable E_s and relatively low dark count, W_c should be optimized, for SPADs with W_m of 1 μm and W_a of 2 μm, the value could be in a range from 0.164 μm to 0.270 μm.

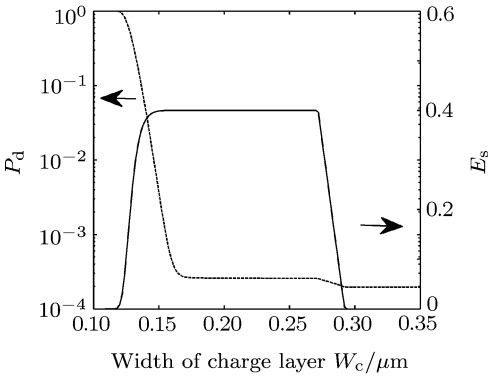


Fig. 5. E_s (right) and P_d (left) of SPAD with 1-μm multiplication layer versus width of charge layer, with an operating temperature of 223 K.

Figure 6 shows P_d increasing with operating voltage. The E_s remains small because the breakdown probability is low and the electric field does not fully deplete the absorption layer when voltage is less than 78 V. When the voltage exceeds 78 V, the absorber is fully depleted and the E_s rises further due to the increase of breakdown probability, but with a smaller slope. As the voltage further increases, the E_s decreases because the increase of the breakdown probability has a less significant effect on E_s than that for the case of P_d. With the optimization of W_c, the maximum value of E_s with W_m of 0.6 μm reaches 0.6129 at a temperature of 223 K. We refer to this maximum value of E_s as the peak E_s.

Figure 7 shows the peak E_s as a function of W_m at temperature of 223 K. The peak E_s greatly rises with W_m increasing, when $W_m < 1$ μm. As W_m further increases, the slope is reduced and the E_s is finally saturated at a quantum efficiency (η) of 0.7433. This phenomenon indicates that an SPAD with W_m

thicker than 1 μm is unnecessary. After all, increasing $W_{\rm m}$ will lead to a larger time jitter.

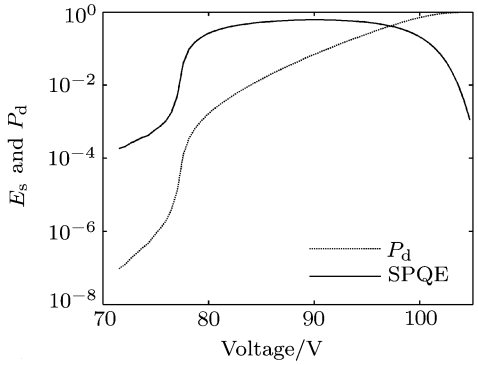


Fig. 6. The $E_{\rm s}$ and $P_{\rm d}$ of SPAD with 0.6-μm multiplication layer versus V at 223 K.

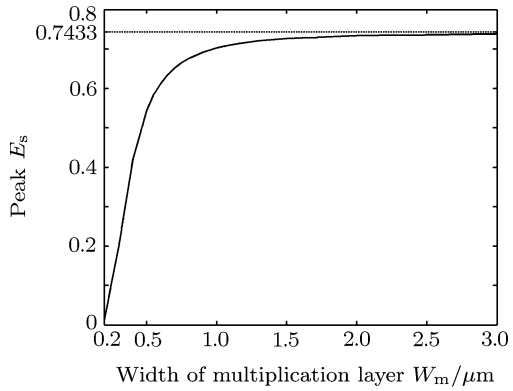


Fig. 7. Peak $E_{\rm s}$ as a function of multiplication layer width at a temperature of 223 K.

4. Discussion

Single photon detections with a high repetition rate have attracted considerable interest recently. In the detection, SPADs are operated at a relatively high temperature, typically -30 °C (243 K).[3] At higher temperatures, the lifetime of trapping carriers is shorter, so the afterpulsing is lower. At higher temperatures, generation–recombination in the absorption layer is the primary dark count mechanism for SPADs with $W_{\rm m}$ around 1 μm, especially when reverse bias is relatively low, because the field dependence of dark count from tunneling is much stronger (exponentially increased).

In order to avoid significant tunneling in absorption layer, the charge layer width $W_{\rm c}$ should be controlled to ensure that the maximum electric field in the absorption layer $E_{\rm a}$ is not too high. On the other hand, the minimum electric field inside the absorber should be higher than that for all photogenerated carriers to drift into multiplication layer with their saturation velocities. We calculated the total dark count probability over the range of $E_{\rm a}$ from 1.0×10^5 V/cm to 2.5×10^5 V/cm. As shown in Fig. 8, $P_{\rm d}$ is almost the same when $E_{\rm a}=1.0\times10^5$ V/cm and $E_{\rm a}=1.5\times10^5$ V/cm. But $P_{\rm d}$ increases abruptly when $E_{\rm a}>1.5\times10^5$ V/cm, and it even exceeds the $E_{\rm s}$ when $E_{\rm a}=2.5\times10^5$ V/cm. This is because the tunneling effects in the charge layer and absorption layer become considerable.

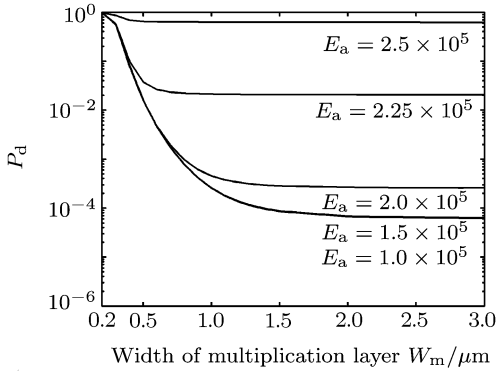


Fig. 8. Curves for $P_{\rm d}$ versus $W_{\rm m}$ for various $E_{\rm a}$ values at temperature of 223 K, with the $E_{\rm s}$ being 0.4.

In order that $E_{\rm s}$ is kept unchanged and $E_{\rm a}$ varies with temperature for a given SPAD, the variation of $E_{\rm a}$ should increase with the decrease of $W_{\rm m}$. An SPAD with a good dark count performance at low temperature may abruptly attain significant a dark count because of the large tunneling in heterojunction when operating at higher temperatures. As an example, an SPAD with $W_{\rm m}$ of 1 μm and $W_{\rm c}$ of 1.9 μm achieves $P_{\rm d}$ of 3.8×10^{-5} at 200 K, but $P_{\rm d}$ reaches 0.026 at 300 K. So we suggest that the SPADs, especially those are employed in the high repetition rates needed to operate at relatively higher temperature, are designed for temperature.

The primary origin of dark counts depends on both device structure and operating condition. Thicker SPADs achieve better $E_{\rm s}$ and dark count performance but with higher time jitter.[9] Thus, an appropriately thick multiplication layer width around 1 μm is recommended to achieve a lower dark count rate and better time performance.

5. Conclusion

A rigorous model is utilized to analyse the $E_{\rm s}$ and the dark count performance of $In_{0.53}Ga_{0.47}As/InP$

SPADs operated in the gate-mode. It is revealed that $P_{\rm d}$ decreases with the increase of multiplication layer width, but the slope decreases gradually and becomes smaller with $W_{\rm m}$. The origin of dark count is investigated. The results indicate that the primary mechanism of dark count depends on both device structure and operating condition. At a temperature of 223 K, band-to-band tunneling in the multiplication layer is the most important mechanism of dark count when 0.2 μm $< W_{\rm m} <$ 1.25 μm. As $W_{\rm m}$ is over 1.25 μm, the generation–recombination in the absorption layer is the dominative mechanism. For an SPAD with 1-μm multiplication layer, when the temperature is higher than 233 K, the dark count from generation–recombination in the absorption layer begins to exceed that from tunneling in the multiplication layer. In addition, when temperature is over 240 K, the generation–recombination in the absorption layer dominates the dark counts.

The charge layer, also called the field control layer, greatly influences the performance of the SPAD by controlling the tunneling and the depletion depth. The peak $E_{\rm s}$ increases with $W_{\rm m}$ and is finally saturated at a certain value of η. The results are heuristic on optimizing the operation of linear APDs used in Geiger mode, as well as on designing and fabricating SPADs specifically for single photon detection at telecom wavelengths.

References

[1] Gisin N, Ribordy G, Tittel W and Zbinden H 2002 *Rev. Mod. Phys.* **74** 145

[2] Ng J S, Tan C H and David J P R 2004 *J. Mod. Opt.* **51** 1315

[3] Namekata N, Sasamori S and Inoue S 2006 *Opt. Express* **14** 10043

[4] Wei Z, Li K, Zhou P, Wang J, Liao C, Guo J, Liang R and Liu S 2008 *Chin. Phys.* B **17** 4142

[5] Wang J, Wu Z, Zhang B, Wei Z, Liao C and Liu S 2008 *Acta Phys. Sin.* **57** 5620 (in Chinese)

[6] Pellegrini S, Warburton R E, Tan L J J, Ng J S, Krysa A B, Groom K, David J P R, Cova S, Robertson M J and Buller G S 2006 *IEEE J. Quantum Electron.* **42** 397

[7] Liu M, Bai X, Hu C, Guo X, Campbell J C, Pan Z and Tashima M M 2007 *IEEE Photon. Technol. Lett.* **42** 378

[8] Jiang X, Itzler M A, Ben-Michael R and Slomkowski K 2007 *IEEE J. Selec. Top. Quantum Electron.* **13** 895

[9] Karve G, Wang S, Ma F, Li X and Campbell J C 2005 *Appl. Phys. Lett.* **86** 063505

[10] Wang S, Ma F, Li X, Karve G, Zheng X and Campbell J C 2003 *Appl. Phys. Lett.* **82** 1971

[11] Sugihara K, Yagyu E and Tokuda Y 2006 *J. Appl. Phys.* **99** 124502

[12] Tan C H, Rees G J, Houston P A, Ng J S, Ng W K and David P R 2004 *Appl. Phys. Lett.* **84** 2322

[13] Yang K, Lu H X, Lo Y H, Bethune D S and Risk W P 2003 *Appl. Phys. Lett.* **83** 2955

[14] Ramirez D A, Hayat M M, Karve G, Campbell J C, Torres S N, Saleh B E A and Teich M C 2006 *IEEE J. Quantum Electron.* **42** 137

[15] Humphreys D A, King R J, Jenkins D and Moseley A J 1985 *IEEE Electron. Lett.* **21** 1187

[16] Karve G 2005 *Ph. D. Thesis* (The University of Texas at Austin, Austin)

[17] Moll J L 1964 *Physics of Semiconductor* (New York: McGraw-Hill)

[18] Forrest S R, Leheny R F, Nahory R E and Pollack W A 1980 *Appl. Phys. Lett.* **37** 322

[19] Sze S Z 1981 *Physics of Semiconductor Devices* 2nd edn. (New York: Wiley)

[20] Hang Z, Shen H and Pollak F H 1990 *Solid State Commun.* **73** 15

[21] Yu P W and Kuphal E 1984 *Solid State Commun.* **49** 907